

Surface-Tuned Assembly of Porphyrin Coordination Oligomers

Matthieu Koepf,[†] Jennifer A. Wytko,^{*,†} Jean-Pierre Bucher,[‡] and Jean Weiss^{*,†}

CLAC, Institut de Chimie de Strasbourg, UMR 7177, CNRS-ULP, 4 rue Blaise Pascal, BP 1032, 67070 Strasbourg, France, and IPCMS, UMR 7504 CNRS-ULP, 23 rue du Loess, BP 43, 67034 Strasbourg, France

Received January 3, 2008; E-mail: jwytko@chimie.u-strasbg.fr, jweiss@chimie.u-strasbg.fr

Abstract: Two self-complementary phenanthroline-strapped porphyrins bearing imidazole arms and C₁₂ or C₁₈ alkyl chains were synthesized, and their surface self-assembly was investigated by atomic force microscopy (AFM) on mica and highly ordered pyrolytic graphite (HOPG). Upon zinc(II) complexation, stable porphyrin dimers formed, as confirmed by DOSY ¹H NMR and UV–visible spectroscopy. In solution, the dimers formed J-aggregates. AFM studies of the solutions dip-coated onto mica or drop-casted onto HOPG revealed that the morphologies of the assemblies formed were surface-tuned. On mica, fiber-like assemblies of short stacks of J-aggregates were observed. The strong influence of the mica's epitaxy on the orientation of the fibers suggested a surface-assisted assembly process. On HOPG, interactions between the alkyl chains and the graphite surface resulted in the stabilization and trapping of monomer species followed by their subsequent association into coordination polymers on the surface. Interdigitation of the alkyl chains of separate polymer strands induced lateral association of wires to form islands that grew preferentially upon drop-casting and slow evaporation. Clusters of laterally assembled wires were observed for the more mobile functionalized porphyrins bearing C₁₂ chains.

Introduction

In the past decade, several examples of photoinduced energy or electron transfer reactions have been reported in geometrically well defined porphyrin dyads, triads, and higher oligomers,^{1,2} and much effort has been devoted to the production of large multiporphyrinic arrays for molecular electronics,³ for electronic^{2,4} or photonic conduction.⁵ On the basis of synthetic considerations, self-assembled multiporphyrin scaffolds appear to have a bright future; however, the controlled formation of quasiinfinite linear arrangements is difficult to achieve, mostly because assembly in solution is entropy controlled.⁶ In addition, before incorporating porphyrin-based materials in operating devices,

the influence of the surface on the assembly of supramolecular nanoobjects needs to be documented as it has been for other self-assembled species.⁷ The results hereafter suggest that surface/object interactions may be used advantageously to direct the self-assembly process.

We have previously reported a phenanthroline-strapped porphyrin that selectively binds imidazole within the phenanthroline strap.⁸ The high association constants ($>10^6$ M⁻¹) observed in chlorinated solvents originate from a combination of weak interactions (metal–ligand coordination, H-bond

[†] CLAC.

[‡] IPCMS.

- (1) (a) Holten, D.; Bocian, D. F.; Lindsey, J. *Acc. Chem. Res.* **2002**, *35*, 57. (b) Harvey, P. D. In *The Porphyrin Handbook*; Kadish, K. M., Smith, K. M., Guillard, R., Eds.; Academic Press: San Diego, 2003; Vol 18, Chapter 113. (c) Wytko, J. A.; Weiss, J. In *N4-Macrocyclic metal complexes*; Zagal, J., ; Bedioui, F., ; Dodelet, J. P., Eds.; Springer: New York, 2006; Vol. 18, pp 63–250. (d) Kobuke, Y. *Struct. Bonding (Berlin)* **2006**, *121*, 4.
- (2) Winters, M. U.; Dahlstedt, E.; Blades, H. E.; Wilson, C. J.; Frampton, M. J.; Anderson, H. L.; Albinsson, B. *J. Am. Chem. Soc.* **2007**, *129*, 4291, and references cited.
- (3) (a) Grill, L.; Dyer, M.; Lafferentz, L.; Persson, M.; Peters, M. V.; Hecht, S. *Nature Nanotechnol.* **2007**, *2*, 687. (b) Satake, A.; Kobuke, Y. *Org. Biomol. Chem.* **2007**, *5*, 1679. (c) Kang, B. K.; Aratani, N.; Lim, J. K.; Kim, D.; Osuka, A.; Yoo, K.-H. *Mater. Sci. Eng., C* **2006**, *26*, 1023. (d) Ayabe, M.; Yamashita, K.; Sada, K.; Shinkai, S.; Ikeda, A.; Sakamoto, S.; Yamaguchi, K. *J. Org. Chem.* **2003**, *68*, 1059.
- (4) (a) Grozema, F. C.; Houamer-Rassin, C.; Prins, P.; Siebbeles, L. D. A.; Anderson, H. L. *J. Am. Chem. Soc.* **2007**, *129*, 13370. (b) Yoon, D. H.; Lee, S. B.; Yoo, K. H.; Kim, J.; Lim, J. K.; Aratani, N.; Tsuda, A.; Osuka, A.; Kim, D. *J. Am. Chem. Soc.* **2003**, *125*, 11062.

- (5) (a) Huijser, A.; Suijkerbuijk, B. M. J. M.; Klein Gebbink, R. J. M.; Savenije, T. J.; Siebbeles, L. D. A. *J. Am. Chem. Soc.* **2008**, *130*, 2485. (b) Balaban, T. S.; Berova, N.; Drain, C. M.; Hauschild, R.; Huang, X.; Kalt, H.; Lebedkin, S.; Lehn, J.-M.; Nifaitis, F.; Pescitelli, G.; Prokhorenko, V. I.; Riedel, G.; Smeureanu, G.; Zeller, J. *Chem. Eur. J.* **2007**, *13*, 8411. (c) Huijser, A.; Marek, P. L.; Savenije, T. J.; Siebbeles, L. D. A.; Scherer, T.; Hauschild, R.; Szymtkowski, J.; Kalt, H.; Hahn, H.; Balaban, T. S. *J. Phys. Chem. C* **2007**, *111*, 11726.
- (6) (a) Lehn, J.-M.; Rigault, A.; Siegel, J.; Harrowfield, J.; Chevrier, B.; Moras, D. *Proc. Natl. Acad. Sci. U.S.A.* **1987**, *84*, 2565. (b) Fujita, M.; Tominaga, M.; Hori, A.; Therrien, B. *Acc. Chem. Res.* **2005**, *38*, 371. (c) Mathias, J. P.; Seto, C. T.; Simanek, E. E.; Whitesides, G. M. *J. Am. Chem. Soc.* **1994**, *116*, 1725.
- (7) (a) Datar, A.; Oitker, R.; Zang, L. *Chem. Commun.* **2006**, 1649. (b) Liu, S.; Wang, W. M.; Mannsfeld, S. C. B.; Locklin, J.; Erk, P.; Gomez, M.; Richter, F.; Bao, Z. *Langmuir* **2007**, *23*, 7428. (c) Stepanow, S.; Lin, N.; Payer, D.; Schlickum, U.; Klappenberger, F.; Zoppellaro, G.; Ruben, M.; Brune, H.; Barth, J. V.; Kern, K. *Angew. Chem., Int. Ed.* **2007**, *46*, 710. (d) Puigmarti-Luis, J.; Minoia, A.; del Pino, A. P.; Ujaque, G.; Rovira, C.; Lledos, A.; Lazzaroni, R.; Amabilino, D. B. *Chem. Eur. J.* **2006**, *12*, 9161. (e) Wu, J.; Watson, M. D.; Zhang, L.; Wang, Z.; Mullen, K. *J. Am. Chem. Soc.* **2004**, *126*, 177.
- (8) Froidevaux, J.; Ochsenbein, P.; Bonin, M.; Schenk, K.; Maltese, P.; Gisselbrecht, J.-P.; Weiss, J. *J. Am. Chem. Soc.* **1997**, *119*, 12362.

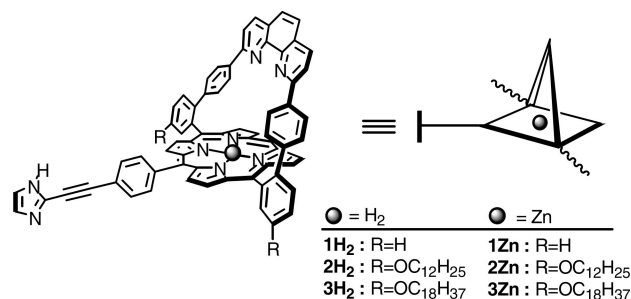


Figure 1. Building blocks for multiporphyrin wires.

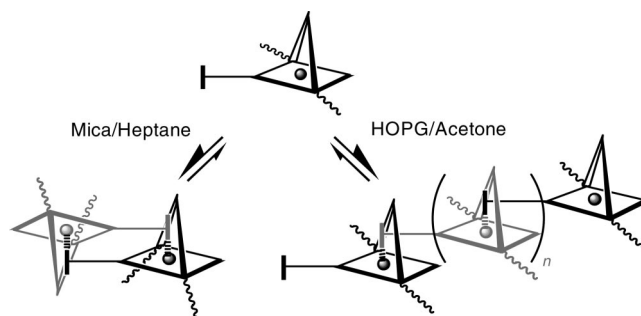
formation, and π - π stacking).⁹ The association of imidazole within the zinc(II) porphyrin is entropy favored due to the loss of two water molecules bound within the strap of the free zinc(II) porphyrin.¹⁰ As a first step toward the preparation of molecular wires, this imidazole recognition was used to design geometrically well defined, self-assembled dyads¹¹ and triads.¹² A second step has now been taken by preparing porphyrins **1Zn**–**3Zn** that self-assemble into oligomers under the proper conditions. The assembly properties and AFM studies of two types of nanoobjects (fibers or wires) obtained from the same molecular species on two different substrates (mica and HOPG) are reported. The results show that the nature of the deposition substrate has a significant impact on the morphology of the resulting objects. Hereafter, wires refer to assemblies with coordination bond connectivity between consecutive monomer units, whereas fibers refer to linear objects formed by aggregation of smaller assemblies that result from weak interactions.

The monomeric units **1H₂**–**3H₂** (Figure 1) were designed such that the formation of long oligomeric or polymeric species was expected to be initiated by insertion of Zn(II) within the porphyrins. Preliminary attempts to metalate **1H₂** with Zn(II) led to insoluble material. This problem was circumvented by anchoring long alkyl chains on the strapped porphyrin framework¹³ to obtain **2H₂** and **3H₂** in good yields (see Supporting Information for synthetic details). Zinc was inserted by treating the free bases **2H₂** and **3H₂** with excess zinc acetate in refluxing THF. The resulting zinc(II) derivatives **2Zn** or **3Zn** were highly soluble in most organic solvents. Initially, linear assembly (Scheme 1, right) was expected because of the unique arrangement previously observed in photochemical triads built on **1-Zn**.¹²

Solution Studies

Solutions of **2Zn** or **3Zn** in halogenated solvents were stable. ¹H NMR DOSY experiments, provided in the Supporting Information (SI Figure S1), of **2Zn** or **3Zn** in deuterated chloroform (5×10^{-4} M CDCl₃) indicated in each case the presence of only one species with relatively large diffusion coefficients of 300 and 250 $\mu\text{m/s}$, respectively. Using an ellipsoidal model and presuming a head-to-tail dimer arrangement as shown on the left in Scheme 1, the large diameter L

Scheme 1. Comparison of Assembly Modes Observed on Mica (left) and on HOPG (right).



(end to end distance between two opposite, fully extended alkyl chains) could be calculated. By fixing the smallest diameter (l) (top of phenanthroline strap to top of phenanthroline strap) at $l = 2$ nm, L was found to be 4.0 nm for **2Zn** and 6.0 nm for **3Zn**, in agreement with respective theoretical values of $L = 3.9$ and 5.5 nm for head-to-tail dimer arrangements, obtained from standard MM2 calculations. An association constant of $K_{\text{assoc}} = 10^9 \text{ M}^{-1}$ in CHCl₃ (see SI Figure S2 for a UV–visible titration) was determined for this dimer formation and contrasts with the association constants in the range of 10^7 M^{-1} usually observed in self-assembled dyads and triads.^{11,12}

UV–visible studies showed that the position of the Soret band was concentration and solvent dependent. In chloroform at concentrations of 5×10^{-5} M and higher, **2Zn** exists primarily as dimers which was also supported by DOSY experiments at similar concentrations (SI Figure S1). The Soret band was observed at 439 nm with a small shoulder at 430 nm, indicating the presence of residual, unbound monomers in solution. Upon dilution to 5×10^{-7} M, the Soret band, with no shoulder, was shifted back to the maximum expected for the four coordinate zinc(II) species at 432 nm (Figure 2). This disappearance of the red-shift is a significant indicator of dissociation and also indicates that only monomers were present in dilute chloroform solutions. In less polar CH₂Cl₂ solutions, **2Zn** and **3Zn** existed as dimers at concentrations of 10^{-7} to 10^{-4} M. Neither the blue shift of the Soret band nor the shoulder on its higher energy side was observed upon dilution. When a 10^{-4} M dichloromethane stock solution of **2Zn** was diluted to 1×10^{-6} M in acetone, the Soret band displayed a broad shoulder at 425 nm and a maximum at 435 nm (SI Figure S3). Therefore, it is assumed that both monomers and dimers of **2Zn** were present in acetone-diluted solution later used for drop-casting deposition on HOPG.

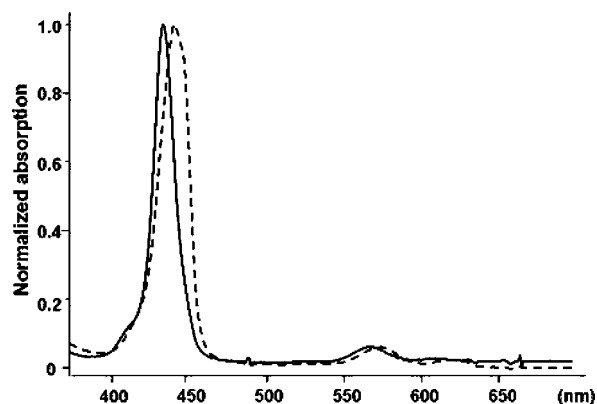


Figure 2. UV–visible spectra of **2Zn** in CHCl₃ at 25 °C: (---) 5×10^{-5} M; (—) 5×10^{-7} M.

- (9) Paul, D.; Melin, F.; Hirtz, C.; Wytoko, J.; Ochsenein, P.; Bonin, M.; Schenk, K.; Maltese, P.; Weiss, J. *Inorg. Chem.* **2003**, *42*, 3779.
 (10) Brandel, J.; Trabolssi, A.; Melin, F.; Elhabiri, M.; Weiss, J.; Albrecht-Gary, A.-M. *Inorg. Chem.* **2007**, *46*, 9534.
 (11) Leray, I.; Valeur, B.; Paul, D.; Regnier, E.; Koepf, M.; Wytoko, J. A.; Boudon, C.; Weiss, J. *Photochem. Photobiol. Sci.* **2005**, *4*, 280.
 (12) Koepf, M.; Trabolssi, A.; Elhabiri, M.; Wytoko, J. A.; Paul, D.; Albrecht-Gary, A.-M.; Weiss, J. *Org. Lett.* **2005**, *7*, 1279.
 (13) Koepf, M.; Melin, F.; Jaillard, J.; Weiss, J. *Tetrahedron Lett.* **2005**, *46*, 139.

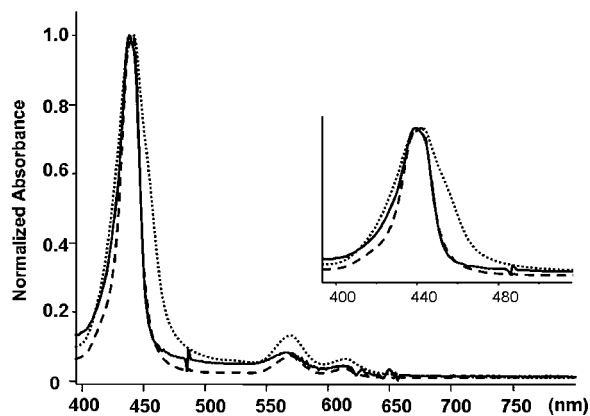


Figure 3. Normalized absorption spectra of **2Zn** at 25 °C: (---) 5×10^{-5} M chloroform solution; (····) initial chloroform solution diluted to 5×10^{-6} M in heptane; (—) initial chloroform solution diluted to 5×10^{-7} M in heptane. The broadening of the Soret band at 440 nm is attributed to the presence of greater π -stacking interaction between dimers induced by the nonpolar heptane. At 5×10^{-7} M, most species are isolated (noninteracting) dimers.

Dilution of chlorinated solutions to micromolar concentrations (10^{-6} M) in heptane afforded slightly red-shifted absorption bands, as shown in the UV–visible spectra in Figure 3. The Soret band was broader with a larger low energy component compared to the Soret in CHCl_3 at 10^{-5} M. Such a combination of broadening and red-shifting suggests a slipped lateral interporphyrin association via π - π stacking that is favored in aliphatic solvents. Furthermore, previous observations of such interactions were found in solid-state structures of strapped porphyrins.¹⁴ Thus, dimers of **2Zn** and **3Zn** must assemble by additional noncovalent interactions into J-aggregates. Further dilution to 10^{-7} M in heptane resulted in a Soret band that was the same as that of the initial chloroform solution. This latter observation is consistent with the loss of dimer–dimer interaction due to dilution and is supported by previous observations that the formation of dimers or higher aggregates not only depends on the intrinsic properties of the molecules but also on external conditions.¹⁵

Solution studies supported the presence of only monomers, dimers, or dimer aggregates, depending on the concentration. The absence of coordination oligomers in solution can be explained by solution thermodynamics in which entropy favors the presence of a larger number of smaller species. These results contrast with those observed in the surface studies presented below.

AFM Studies

To investigate the aggregation tendency observed in solution, AFM studies were undertaken based on previous reports of the surface deposition of J-aggregates and their ability to form higher assemblies on substrates.¹⁶ Noncontact mode AFM studies showed that identical species can exhibit markedly different and reproducible behaviors regarding their self-assembly during a surface-tuned process. Deposition of **2Zn** or **3Zn** was carried out in various solvents ($\sim 1 \mu\text{M}$) by vertical dipping of freshly cleaved mica or drop-casting on HOPG. In

the case of dip coating, the excess solvent was blotted off prior to air drying. For drop casting, the sample was air-dried or exposed to a vapor saturated atmosphere.

Both dip-coating and drop-casting methods of deposition were preliminarily tested to determine the best method for each substrate (detailed procedures in SI, page S10). In the case of mica, the following solvents were tested: acetone, dichloromethane, heptane, and THF. Dip-coating procedures generated suitable samples and organized assemblies only when heptane solutions were used. By drop-casting, assemblies similar to those observed by dip-coating were observed only when the drop of solution was allowed to evaporate slowly in a heptane-saturated atmosphere. Thus, for mica deposition, only results obtained by dip-coating will be presented. The same solvents as well as dioxane were tested for deposition onto HOPG, but samples generated by dip-coating were poorly reproducible and hardly exploitable. Drop-casting gave more interesting preliminary results and was therefore pursued in more detail.

AFM Studies on Mica. Using tips with a typical curvature radius of 10–12 nm on mica, we observed regular arrangements of linear assemblies of **2Zn**, as shown in Figure 4. Although other types of assemblies were occasionally observed (SI Figure S4), the images in Figure 4 were highly reproducible and best represent structures that were observed over most of the substrate. A strong influence of mica's hexagonal epitaxy was visible in the orientation of the assemblies (Figures 4b–d), as well as in the 2-D fast Fourier transform (FFT) (middle column Figures 4b–d). As a result of the dip-coating deposition method, the size distribution of the objects varied depending on the area of the substrate explored (Figure 4).

The length of the objects increased going from the top of the mica support to the bottom. Within the same horizontal zone (a, b, c, or d in Figure 4), the assemblies were relatively homogeneous. Objects near the top of the support (Figure 4a) had an average length of 30 nm, whereas those closer to the bottom (Figure 4d) averaged 204 nm in length. The size of self-assembled structures on surfaces is known to be concentration dependent,¹⁷ which, because of the deposition method, is consistent with the observation of longer fibers near the bottom of the mica support.

At the top of the support (Figure 4a), 70% of the small aggregates observed were shorter than 25 nm long. Several millimeters lower on the support (Figure 4b), short fibers covered the surface. In this zone, 70% of the objects were > 25 nm long in at least one direction. The influence of mica's hexagonal epitaxy was already visible in this second zone. When an area in the bottom half of the support was explored (Figure 4c), fibers that measured 43–209 nm in length were observed. The length of 70% of the objects was > 70 nm. The longest strands were present at the bottom of the mica support (Figure 4d), where 70% of the fibers were longer than 110 nm. In this area, the orientation of longest fibers was more random.

To investigate whether or not the length of the alkyl chains played a role in the type of objects formed on mica, **3Zn** with C_{18} chains was studied under the same condition as for **2Zn**. Compound **3Zn** was also deposited on mica supports by dip-coating the support in a $1 \mu\text{M}$ heptane solution of **3Zn** for 15 s. As shown in Figure 5, deposits of nonorganized material and small films were observed near the top of the mica support (Figures 5a,b), whereas complex networks of fiber-like struc-

(14) Melin, F.; Boudon, B.; Lo, M.; Schenk, K. J.; Bonin, M.; Ochsnein, P.; Gross, M.; Weiss, J. J. *Porphyrins Phthalocyanines* **2007**, *11*, 212.

(15) For examples of distinct monomer-dimer equilibria of dye aggregates see Wurthner, F.; Yao, S.; Debaerdemaeker, T.; Wortmann, R. *J. Am. Chem. Soc.* **2002**, *124*, 9431.

(16) Balaban, T. S. *Acc. Chem. Res.* **2005**, *38*, 612.

(17) Guo, Q.; Yin, J.; Palmer, R. E.; Bampos, N.; Sanders, J. K. M. *J. Phys.: Condens. Matter* **2003**, *15*, S3127.

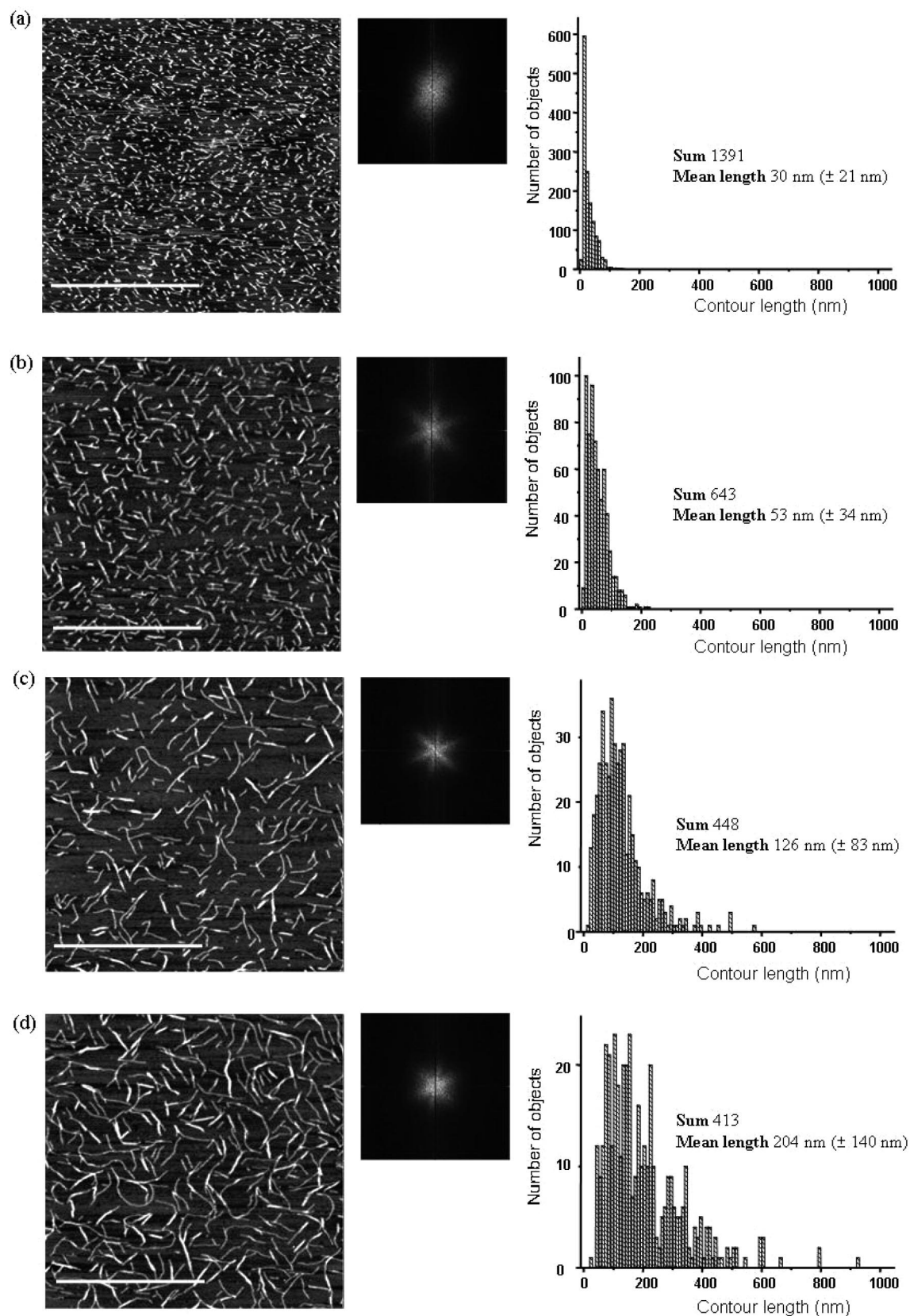


Figure 4. Influence of the position explored on mica on the morphology of species formed by dipping a support in a $\sim 1 \mu\text{M}$ heptane solution of 2Zn for 15 s. Left column: topographic images; middle column: 2-D FFT; right column: length distribution histograms. (a) Top edge of support; (b and c) intermediate positions of mica support; (d) bottom edge of support. The histogram of each image represents the contour length distribution of species observed on the mica surface. For positions c and d, the histograms and the average length measurements were based on several images, taken on the same horizontal line. Scale bar: $1 \mu\text{m}$; vertical scale: 6 nm.

tures, similar in height to the fibers observed for 2Zn (see the following section), tended to form at the bottom of the support

(Figures 5c,d). Mica's epitaxy was found to be less pronounced on the orientation of the fibers formed from 3Zn than from 2Zn ,

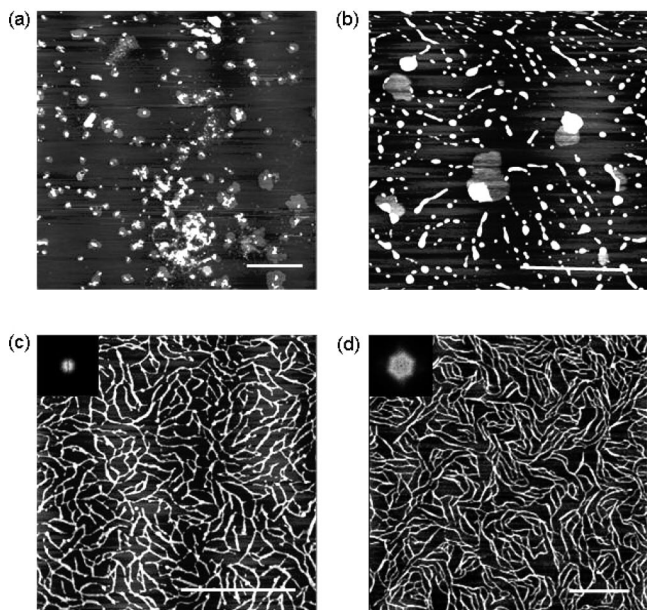


Figure 5. AFM images of **3Zn** dip-coated onto mica. Mica supports were dipped for 15 s into a 1 μ M heptane solution of **3Zn**. (a and b) Top area of mica support. (c and d) Bottom area of the support. Scale bar: 1 μ m; vertical scale: 5 nm.

as exemplified by the more uniform dispersion of frequencies in 2D-FFT spectra (insets in Figures 5c,d). These observations are consistent with an erratic contribution of a spinodal dewetting phenomenon that is widely used to explain self-organization and molecular ordering on various surfaces,^{18–22} including the case of porphyrin species.^{17,23,24}

It should be noted that spinodal dewetting patterns are less frequently observed for the C_{12} -appended **2Zn** structure than for the C_{18} -appended **3Zn**. In the case of **2Zn**, dewetting patterns were observed on very small, localized sections of the substrates (SI Figure S4), but the corresponding images were not representative of the assemblies observed over the major portion of the substrates. The low occurrence of random distribution (as opposed to aligned patterns) of the assemblies demonstrates that in our case, in heptane, spinodal dewetting does not play an important role in the formation of assemblies.²⁵ Furthermore, the fast Fourier transforms shown in Figures 4b–d are atypical of spinodal dewetting²⁶ and show a pronounced influence of mica's epitaxy.

Fine Structure and Organization of 2Zn Assemblies on Mica. Because of their greater homogeneity over a larger surface of deposition, assemblies produced from **2Zn** were selected for more detailed investigation. The fine structure of fibers formed

from **2Zn** could be seen on detailed AFM images such as those in Figure 6. Better resolved images were obtained using AFM super sharp tips with a much lower curvature radius (2–3 nm). The high resolution images showed that the fibers were fragmented rather than continuous, suggesting that the fibers were formed by lateral association of smaller, linear segments that were spaced 4.5 ± 0.5 nm apart for the most compact arrangements (Figures 6b and 6c). The most homogeneous fibers were observed when each linear segment adopted an orientation parallel to its neighboring segments and perpendicular to the axis of the fiber.

The assemblies in Figure 6 measured between 8–21 nm in width and 1.63 ± 0.43 nm in height. The dimensions of a **2Zn** dimer (Figure 7) calculated with ChemDraw 3D are 3.85 nm \times 1.62 nm (Figure 7). The width of the dimer (1.6 nm) is the only calculated dimension that matches the height of the objects (1.63 ± 0.43 nm) observed on mica. This observation suggests the edge-on deposition of objects that are primarily formed in solution (Figure 7). The width of the linear objects did not match any of the calculated dimensions of the dimer; therefore, additional structuring interactions were considered.

We propose that the formation of the objects thus starts with the J-type aggregation of dimers (Figure 7c) present in the initial 1 μ M heptane stock solution used for dip coating. Small stacks of four to five dimers are then deposited edge-on onto the surface, thus allowing association of their lipophilic contours and minimization of unfavorable interactions with the hydrophilic surface. The progressive increase in the size of the objects toward the bottom of the plate and their orientation with respect to a 6-fold symmetry suggest that growth into larger assemblies occurs on the surface and is mostly directed by the crystallographic symmetry of mica surface (epitaxial growth). The dependency of assembly orientation on the epitaxy may be due to interactions between the phenolic oxygens and the potassium cations present on the mica surface. Contact between the solution and substrate was the longest at the bottom of the plate, where solution was still visible for 20–30 s after the residual drop was absorbed with paper. Therefore, the small assemblies already present on the substrate maintain their mobility for a longer period, allowing extended assemblies to form. Interestingly, the number of small aggregates observed diminished as longer fibers were observed on the plate. Such a seeding effect of porphyrin stacks has been proposed to explain the growth of large lamellar porphyrin assemblies on HOPG.²⁷

AFM of 2Zn and 3Zn on HOPG. Based on the established stabilizing effect of alkyl chains on HOPG,²⁸ AFM studies of **2Zn** and **3Zn** deposited on lipophilic HOPG surface were undertaken. Acetone and dioxane were chosen for in-depth AFM studies on HOPG because these solvents initially demonstrated the best wetting ability and produced the highest degree of homogeneity of assemblies on the graphite surface. Both the behavior and the growth process of the objects obtained from **2Zn** or **3Zn** on HOPG (Figure 8) are strikingly different from those observed on mica. Drop-casting deposition and air evaporation of 0.5 μ M acetone solutions of **2Zn** on HOPG produced short linear objects (Figure 8a) that were 13–18 nm wide, 20–40 nm long, and 1.26 ± 0.09 nm high. These objects were consistently shorter than the fibers observed on mica. Under similar deposition conditions, **3Zn** led to slightly longer

(18) Müller-Buschbaum, P. J. *Phys.: Condens. Matter* **2003**, *15*, R1549.

(19) Sferrazza, M.; Heppenstall-Butler, M.; Cubitt, R.; Bucknall, D.; Webster, J.; Jones, R. A. L. *Phys. Rev. Lett.* **1998**, *81*, 5173.

(20) Higgins, A. M.; Jones, R. A. L. *Nature* **2000**, *404*, 476.

(21) Moriarty, P.; Taylor, M. D. R. *Phys. Rev. Lett.* **2002**, *89*, 248303.

(22) Sharma, A.; Khanna, R. *Phys. Rev. Lett.* **1998**, *81*, 3463.

(23) van Hameren, R.; Schön, P.; van Buul, A. M.; Hoogboom, J.; Lazarenki, S. V.; Gerristen, J. W.; Engelkamp, H.; Christianen, P. C. M.; Jeus, H. A.; Maan, J. C.; Rasig, T.; Speller, S.; Rowan, A. E.; Elemans, J. A. A. W.; Nolte, R. J. M. *Science* **2006**, *314*, 1433.

(24) van Hameren, R.; van Buul, A. M.; Castriciano, M. A.; Villari, V.; Micali, N.; Schön, P.; Speller, S.; Monsù Scolaro, L.; Rowan, A. E.; Elemans, J. A. A. W.; Nolte, R. J. M. *Nano Lett* **2008**, *8*, 253.

(25) An insignificant role of spinodal dewetting was suggested in the case of *n*-hexane solutions on mica in ref 24.

(26) FFT of spinodal dewetting processes are spherical. See ref 21.

(27) Zhou, Y.; Wang, B.; Zhu, M.; Hou, J. G. *Chem. Phys. Lett.* **2005**, *403*, 140.

(28) (a) Tao, F.; Bernasek, S. L. *Chem. Rev.* **2007**, *107*, 1408. (b) De Feyter, S.; De Schryver, F. C. *Chem. Soc. Rev.* **2003**, *32*, 139.

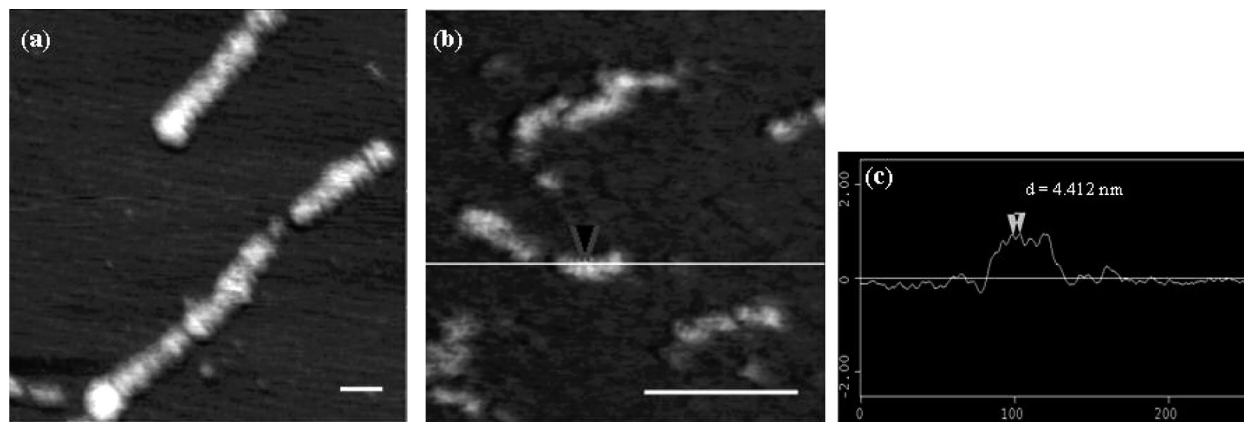


Figure 6. (a and b) Details of **2Zn** fibers. (c) Cross-section taken from image b (white line). Sample obtained by dip-coating a mica sample in a $\sim 1 \mu\text{M}$ heptane solution of **2Zn** for 15 s. AFM tips with a typical radius of 2–3 nm were employed to increase the resolution. Scale bar: 100 nm; vertical scale: 5 nm.

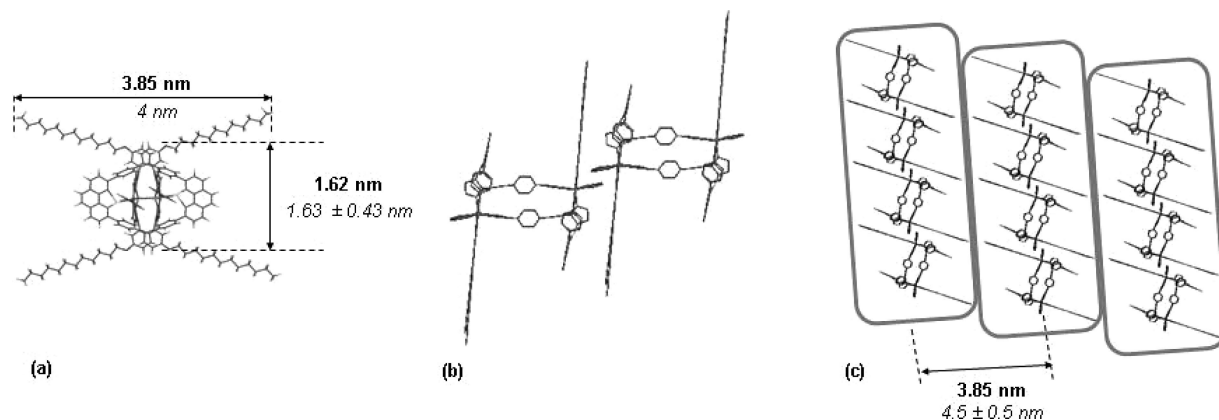


Figure 7. Representation and dimensions of dimer **2Zn** and its proposed organization on mica. (a) Profile and theoretical dimensions (in bold) of **2Zn** dimer. The measured height of the assemblies on the mica surface is given in italic. The large diameter of the dimer determined by DOSY NMR calculations is given in italic. (b) Proposed assembly of **2Zn** dimers. (c) Proposed orientation and assembly mode of strands of dimers on the mica surface (top view) and indication of the theoretical periodicity for an assembly without intercalation of the lipophilic chains. Theoretical values are given in bold, and values measured from the AFM images are given in italic.

linear objects and more aggregation (Figure 8d) than for **2Zn**. The linear objects formed from **3Zn** were 15–19 nm wide and 1.25 ± 0.22 nm high.

When acetone solutions were evaporated more slowly in a solvent-saturated atmosphere, a higher degree of association was observed. For **3Zn**, the lateral assembly of wires was observed, as shown in Figures 8e and 8f (circled objects). Under the same deposition conditions, **2Zn** formed small islands of film as seen in Figure 8b via progressive lateral association of objects depicted in Figure 8c. These islands are reminiscent of assemblies observed for zinc porphyrins bearing four methyl ester side chains and two (trimethylsilylethynyl)phenyl groups.¹⁷

Organization of 2Zn and 3Zn on HOPG. The heights of assemblies of **2Zn** and **3Zn** on HOPG were respectively 1.26 ± 0.09 and 1.25 ± 0.22 nm. These values measured on isolated linear objects are 0.4–0.5 nm smaller than those observed for the same assemblies on mica, suggesting a different mode of organization. The theoretical distance from the phenolic oxygen to the top of the phenanthroline strap was calculated to be 1.25 nm using Chem 3D standard modeling. The correspondence between calculated height and the observed AFM heights of the objects indicates that the isolated linear objects and films were a single molecule thick. Thus, it is proposed that the porphyrins lie flat on the graphite surface with C₁₂ or C₁₈ alky chains to either side, as depicted in Figure 9. In this way,

interactions are always maximized between the lateral side chains and the graphite surface.

In larger aggregates in which individual linear wires were distinct, such as the circled assemblies of **3Zn** in Figure 8e, the lowest measurable center-to-center distance between two wires was 9 nm (SI Figure S5). This distance characterizes an assembly assigned to an intermediate situation between isolated linear wires and the islands of films formed by lateral interdigitation of alkyl side chains. The interdigitation of alkyl chains would be characterized by distances shorter than 6 nm for **3Zn**, and less than 5 nm for **2Zn**. Such short spacing was not observed in the islands of films, suggesting that a very compact arrangement is reached (SI Figure S6). In this higher degree of organization the height of the islands was highly uniform, with no distinguishable individual segments, and no corrugation. Such a uniform aspect confirmed that individual segments (wires) were in close proximity.

Thus, contrary to the situation with heptane and mica in which the hydrophilic surface forces a solution self-assembly process, the affinity of the side chains and of the porphyrin's flat lipophilic surface for HOPG leads to a complete surface-assisted self-assembly process. At submicromolar concentrations in acetone, dimers are mostly dissociated, as described above. Thus, the formation of coordination polymers takes place *a posteriori* to the deposition of mobile isolated monomers onto

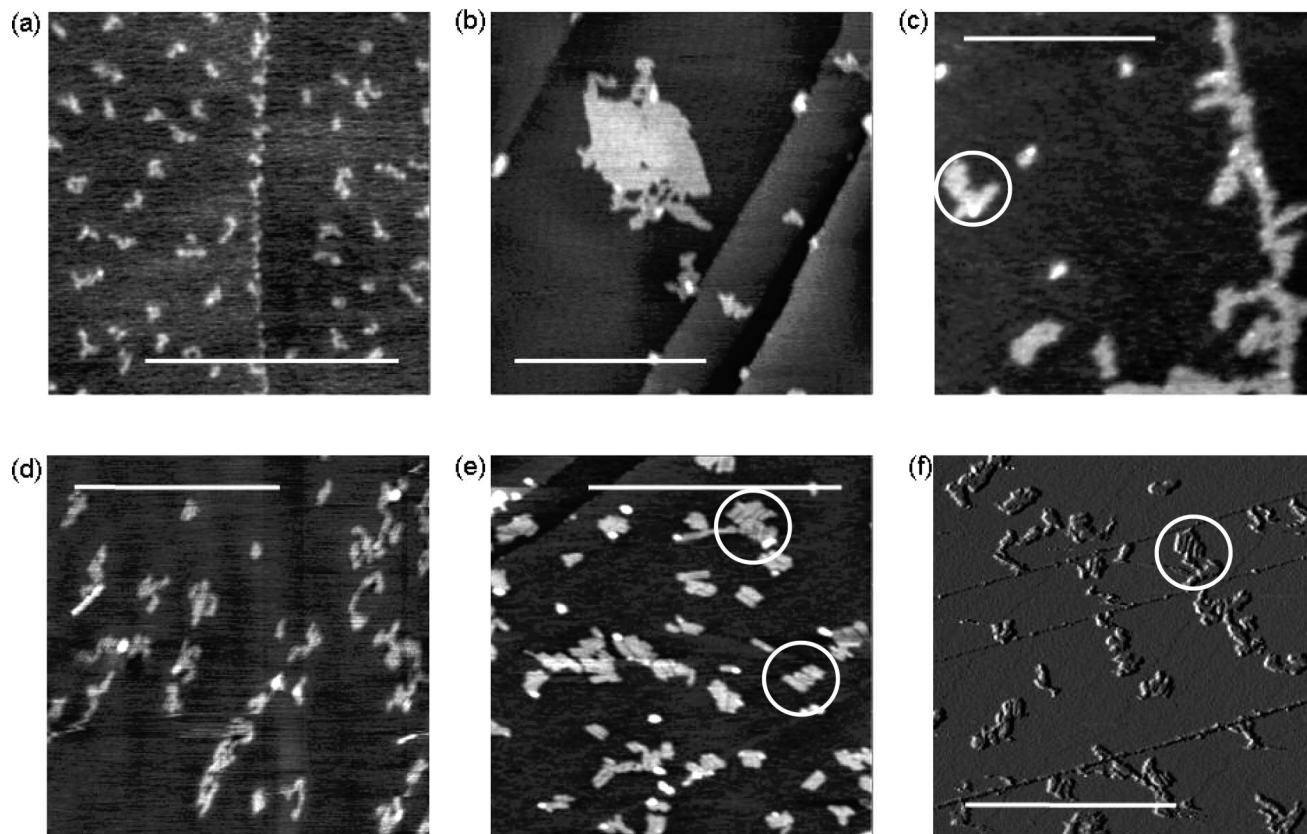


Figure 8. AFM images of **2Zn** and **3Zn** drop-casted ($0.5 \mu\text{M}$ in acetone) onto HOPG: (a) **2Zn** evaporation in air; (b) **2Zn** slow evaporation in an acetone saturated atmosphere; (c) **2Zn** slow evaporation in an acetone saturated atmosphere: detail of the lateral aggregation process; (d) **3Zn** evaporation in air; (e and f) **3Zn** slow evaporation in an acetone saturated atmosphere. Amplitude image (deflection scale = 0.02 V) that illustrates the side by side aggregation of **3Zn**. Scale bar: 500 nm ; vertical scale: 5 nm .

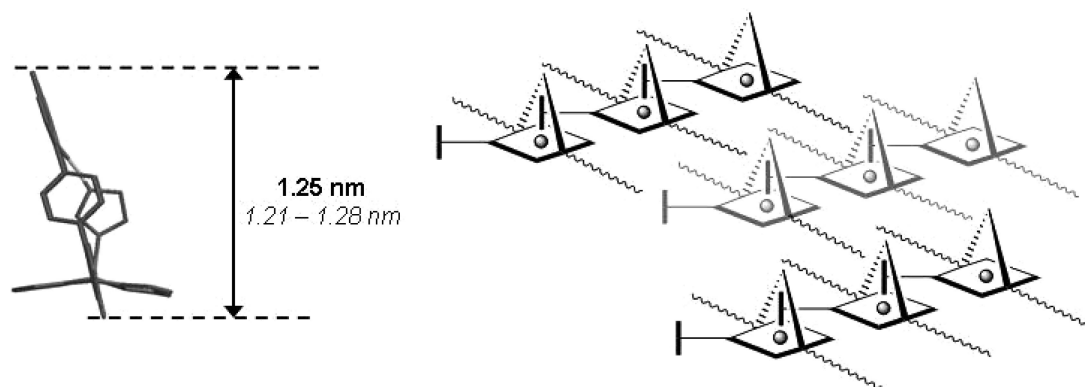


Figure 9. Calculated height (in bold) and proposed mode of assembly of **2Zn** or **3Zn** on HOPG. Typical height range observed by AFM is given in italic.

the HOPG surface. Thus, the assembly process begins when the imidazole arm of one monomer is bound within the phenanthroline strap of a second monomer that is sufficiently close to the first monomer. The assembly process continues in this manner until complete evaporation of the solvent. Accordingly, it would be expected that monomers with a moderate affinity for HOPG would preserve some mobility over a longer period of time than monomers with a higher affinity, especially when slow evaporation proceeds under a solvent saturated atmosphere.

This hypothesis is supported by comparison of the aggregates of **2Zn** and **3Zn** formed by evaporation in an acetone-saturated atmosphere. Whereas small islands of oriented films were

observed for **2Zn** (Figure 8b), only small groups of laterally assembled wires were visible for **3Zn** (Figure 8e). The relatively small size of the islands of film in Figure 8b was probably caused by fast evaporation of acetone (bp $56 \text{ }^\circ\text{C}$). The concomitant lower occurrence of small objects on the surrounding HOPG steps confirms that the short C_{12} functionalized linear segments tend to be mobile on the surface. Assemblies of **3Zn** with longer C_{18} side chains should intuitively have a greater affinity than **2Zn** for the graphite surface. The absence of island formation for **3Zn** that is evaporated slowly in acetone-saturated atmosphere is probably due to the reduced mobility.

Further confirmation that aggregate size is mobility dependent comes from the observation of films of **2Zn** formed by slow

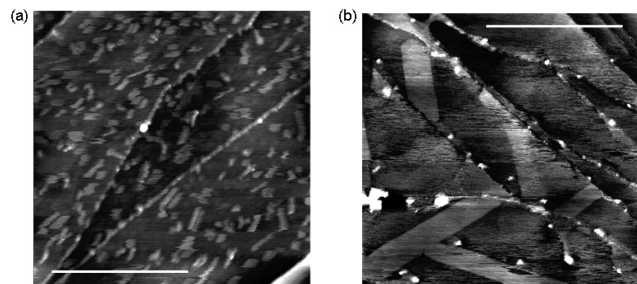


Figure 10. AFM images of **2Zn** in dioxane drop-casted on HOPG: (a) evaporation in air; (b) evaporation in a dioxane saturated atmosphere. Scale bar: 500 nm. Vertical scale: 6 nm.

evaporation of drop-casted dioxane solutions on HOPG (Figure 10b). By using dioxane, a less polar (0.45 D) and less volatile (bp 102 °C) solvent, the mobility of the coordination polymer segments was maintained over a longer period, allowing larger films to form (thickness = 1.25 ± 0.22 nm). In this case, almost no isolated short segments were seen on the surface. The evolution of organization as a function of the species' mobility is reminiscent of that reported by Otsuki for tripod molecules bearing long alkyl side chains.²⁹

Conclusion

Molecular recognition by combined weak interactions is often used to obtain self-corrected assembly of materials.³⁰ The incorporation of self-assembled materials onto patterned surfaces

(29) Otsuki, J.; Shimizu, S.; Fumino, M. *Langmuir* **2006**, *22*, 6056.

(30) During the course of this work, a similar iterative approach using axial base coordination in mutated hemoprotein was reported. Kitagishi, H.; Oohora, K.; Yamaguchi, H.; Sato, H.; Matsuo, T.; Harada, A.; Hayashi, T. *J. Am. Chem. Soc.* **2007**, *129*, 10326.

will raise problems related to the perturbation of these interactions by molecule/surface interactions. These results show how interactions between a surface and molecules can influence the self-assembly process. In solution, porphyrins **2Zn** and **3Zn** both exist as dimers that form J-aggregates. When deposited on mica, the dimer and J-aggregate structures remain intact and assemble into larger fibers by weak intermolecular interactions. On HOPG, favorable CH- π interactions between the porphyrins' long alkyl side chains and the graphite surface prevent dimer formation and favor the association of monomers into linear coordination polymers. In the prospect of incorporating self-assembled molecular materials on patterned surfaces, recent results emphasize the surface-molecule interactions as a crucial parameter to control.³¹ This series of self-assembling strapped porphyrins represent ideal candidates for a systematic exploration of side chain effects on the growth of monomolecular films which is under progress.

Acknowledgment. M.K. is grateful to the Région Alsace and the CNRS for a Ph.D. fellowship. We are grateful to Dr. M. Elhabiri for calculation of the association constant for **2Zn** dimer. This work was supported by the CNRS (ACI-NX001) and Research Council of the Université Louis Pasteur.

Supporting Information Available: Synthetic and surface deposition procedures, DOSY NMR, K_a determination by UV-visible spectroscopy, UV-vis of **2Zn** in CH_2Cl_2 , acetone, and CHCl_3 , and occasionally observed AFM images of **2Zn** on mica are provided free of charge via the Internet at <http://pubs.acs>.

JA800039A

(31) Wei, Y.; Tong, W.; Zimmt, M. B. *J. Am. Chem. Soc.* **2008**, *130*, 3399.